Int. J. Heat Mass Transfer. Vol. 14, pp. 513–520. Pergamon Press 1971. Printed in Great Britain

VELOCITY PROFILES IN TWO INTERDIFFUSING GAS STREAMS

G. WYATT

Thermal and Fluid Sciences Center, Institute of Technology, Southern Methodist University, Dallas, Texas, U.S.A.

W. E. IBELE and E. R. G. ECKERT

Heat Transfer Laboratory, Mechanical Engineering Department, University of Minnesota, Minneapolis, Minnesota, U.S.A.

(*Received* 22 *December* 1969 *and in revised form* 15 *June* 1970)

Abstract—Experimental velocity profiles are presented for tube flow in which a strong concentration gradient occurs in a binary gas mixture. With convective and diffusive velocities of approximately the same size, the velocity profiles are markedly different from the parabolic profiles ordinarily expected and may exhibit a minimum along the centerline of the tube. A concentration profile from first order diffusion theory is used with a power series to produce an approximate axial velocity distribution.

NOMENCLATURE

A, B, C, D',	coefficients in velocity profile; functions of the axial coordinate, y;
D,	mass diffusion coefficient;
F,	dimensionless flow parameter defined in equation (1);
L,	total length of diffusion chamber;
$\dot{m}$,	mass flow rate per unit area;
M,	molecular weight;
P,	pressure;
r,	radial coordinate;
R,	radius of diffusion chamber;
$\bar{R}$,	universal gas constant;
T,	temperature;
u,	convective axial velocity;
v,	convective radial velocity;
w,	mass concentration;
x,	mole concentration;
y,	axial coordinate;
Y,	dimensionless distance y/L;
α,	thermal diffusion factor;
ρ,	density.

Subscripts

0,	average quantity at $y = 0$;
1,	heavy gas;
2,	light gas;
12 or 21,	mixture of gas 1 and 2.

INTRODUCTION

THE VELOCITY of a fluid flowing in a pipe has been examined analytically and experimentally by many investigators. Thus it is established that velocity profiles occur in tubes which differ considerably from those occuring under laminar isothermal, viscous flow conditions. The effect of a radial temperature gradient can be particularly significant because of the influence of temperature on the coefficient of viscosity for many fluids [1]. The current work is unique because the diffusion process causes a marked change from the ordinarily expected parabolic profile. This occurs because the diffusive velocity in the test section is the same order of magnitude as the convective velocity.

The results of a simple experiment, show that whenever a strong concentration gradient occurs in a binary gas mixture with convective and diffusive velocities of approximately the same size, the velocity profile is distorted from that expected.

STATEMENT OF PROBLEM

The physical situation is shown in Fig. 1.

The two interdiffusing gases are denoted by 1 and 2; 1 denotes the heavier gas and 2 the lighter gas. Gas 2 is admitted into the upper section of a vertical tube divided into two regions by a porous

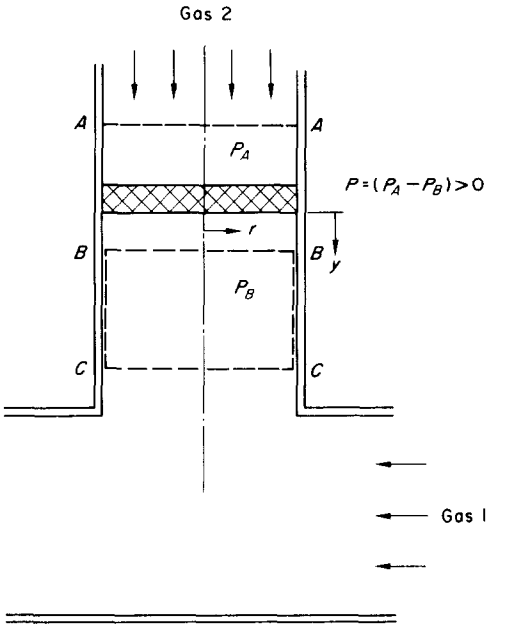

FIG. 1. Physical model and coordinates.

material. Gas 1 flows through a rectangular duct normal to the vertical tube. The porous material causes a pressure drop to gas 2 which acts to prevent gas 1 from reaching the region above the porous material in any significant quantity.

A concentration gradient is established in the lower region of the tube and a diffusive mass flow results. The analysis is simplified by assuming and subsequently verifying that concentration varies primarily only in the vertical direction. The relation giving the concentration as a function of vertical distance may be derived by considering mass flow through the cross section B–B in Fig. 1. The mass flow of gas 2 per unit time and area is given by

$$\dot{m}_2 = -\rho D_{21}\frac{dw_2}{dy} - \rho D_{21} w_1 w_2(\alpha)_{21}\frac{\partial \ln T}{\partial y} + \rho w_2 u. \quad (1)$$

A similar equation may be written for gas 1 as:

$$\dot{m}_1 = -\rho D_{12}\frac{dw_1}{dy} - \rho D_{12} w_1 w_2(\alpha)_{12}\frac{\partial \ln T}{\partial y} + \rho w_1 u. \quad (2)$$

In both equations (1) and (2) the w's and α are of order of magnitude one and dw/dy and $\partial T/\partial y$ have the same order of magnitude. The thermal diffusion term can then be neglected since

$$\frac{dw}{dy} \gg w_1 w_2(\alpha)\frac{\partial \ln T}{\partial y}.$$

Equations (1) and (2) then reduce to:

$$\dot{m}_2 = -\rho D_{21}\frac{dw_2}{dy} + \rho w_2 u \quad (3)$$

and

$$\dot{m}_1 = -\rho D_{12}\frac{dw_1}{dy} + \rho w_1 u. \quad (4)$$

By integrating over the cross sectional area and then dividing by the area

$$\overline{\dot{m}_2} = -\rho D_{12}\frac{d\overline{w_2}}{dy} + \rho w_2 \bar{u} \quad (5)$$

and

$$\overline{\dot{m}_1} = -\rho D_{21}\frac{d\overline{w_1}}{dy} + \rho w_1 \bar{u} \quad (6)$$

where the bar indicates average quantities. Now the line connected to the vertical cylinder through which gas 2 enters leads only to a high pressure commercial gas bottle; thus under steady state conditions no net flow of gas 1 can occur across plane B–B. In equation (6) $\overline{\dot{m}_1}$ may be set equal zero and since

$$\frac{d\overline{w_1}}{dy} = \frac{dw_1}{dy}$$

$$\bar{u} = \frac{D_{21}}{w_1}\frac{dw_1}{dy}. \quad (7)$$

Equation (5) may now be modified by using equation (7), the kinetic theory relation, $D_{12} = D_{21}$, and the relations

$$w_1 + w_2 = 1$$

and

$$\frac{dw_1}{dy} = -\frac{dw_2}{dy}$$

as:

$$\bar{\dot{m}}_2 = \frac{\rho D_{12}}{w_1}\frac{dw_1}{dy}. \tag{8}$$

Using the ideal gas law $\rho = PM/\bar{R}T$ and the relations between mass and mole fraction,

$$w_1 = \frac{x_1 M_1}{M}$$

and

$$\frac{dw_1}{dy} = \frac{M_1 M_2}{M_2}\frac{dx_1}{dy},$$

the molar form of the mass flux equation is

$$\bar{\dot{m}}_2 = D_{12}\frac{PM_2}{T\bar{R}}\frac{d(\ln x_1)}{dy}. \tag{9}$$

This may be integrated and rearranged as:

$$x_1 = x_{1,0}\, e^{FY} \tag{10}$$

where

$$F = \frac{\bar{\dot{m}}_2 T\bar{R}L}{D_{12}PM_2},$$

a dimensionless parameter with $Y = y/L$, and $x_{1,0}$ is the concentration of gas 1 at $y = 0$.

Analytical approximation

The Navier–Stokes equations for a viscous compressible fluid describe the flow field in this problem. These equations will, however, not be used since they contain variable properties and are rather complex. An approximate solution is obtained in the following way. An approximate profile is an even function in r of the form

$$\frac{u(r, y)}{u_0} = A(y) + B(y)\, r^2 + C(y)\, r^4. \tag{11}$$

With this assumed form

$$\left(\frac{\partial u}{\partial r}\right)_{r=0} = 0$$

is satisfied.

The boundary conditions which are useful are:

(1) $u(R, y) = 0$,
i.e. fluid at wall is stationary (12).

(2) $\bar{u} = \frac{D_{12}}{w_1}\frac{dw_1}{dy}$, i.e. equation (7)

(3) An additional condition is obtained by consideration of the continuity equation:

$$\frac{\partial}{\partial y}(\rho r u) + \frac{\partial}{\partial r}(\rho r v) = 0. \tag{13}$$

For the current problem, since ρ is not a function of r, this may be expanded as:

$$\frac{\partial}{\partial y}(\rho u) = -\frac{\rho}{r}\left[v + r\frac{\partial v}{\partial r}\right]. \tag{14}$$

It is known that at $r = 0$, $v = 0$, and there is no diffusion in the radial direction since $\partial w_1/\partial r = 0$. As an approximation it is then assumed that

$$\left.\frac{\partial v}{\partial r}\right|_{r=0} = 0. \tag{15}$$

This in turn gives

$$\left.\frac{\partial}{\partial y}(\rho u)\right|_{r=0} = 0. \tag{16}$$

(This is shown to be a good approximation by a comparison of the calculated profiles and experimental data.) The additional condition

$$\frac{u(r, 0)}{u_0} = -2\left(\frac{r^2}{R^2} - 1\right), \tag{17}$$

where u_0 is the average velocity entering the test section, reduces the profile to the parabolic form on entry into the test section and allows the elimination of the integration constant involved with equation (16).

The axial velocity may then be approximated by the application of these conditions to equation (11). The first condition gives:

$$A(y) = -B(y)R^2 - C(y)R^4. \tag{18}$$

Using equation (18) in equation (11) and averaging the axial velocity over the cross section B–B results:

$$\frac{\bar{u}}{u_0} = -B(y)\frac{R^2}{2} - C(y)\frac{2R^4}{3}. \tag{19}$$

Equation (19) may be used to determine $B(y)$ as a function of $C(y)$. At this point with $A(y)$ and $B(y)$ eliminated from equation (11) the axial velocity is:

$$\frac{u}{u_0} = -\frac{2\bar{u}}{u_0R^2}(r^2 - R^2) + C(y)\left\{r^4 - R^4 - \frac{4R^2}{3}(r^2 - R^2)\right\}. \tag{20}$$

If equation (16) is applied to equation (20) and the result integrated with respect to y:

$$C(y) = -(\rho\bar{u} + D')\left(\frac{6}{\rho u_0 R^4}\right) \tag{21}$$

where D' is a constant since the other terms of equation (21) depend only on y. This constant may be determined by considering that at y equal zero $\bar{u} = u_0$, $\rho = \rho_0$, and equation (17). This gives $D' = -\rho_0 u_0$ and the axial velocity is then completely known:

$$\frac{u(r, y)}{u_0} = \frac{-2\bar{u}}{u_0R^2}(r - R^2) - \frac{6}{R^4}\left(\frac{\bar{u}}{u_0} - \frac{\rho_0}{\rho}\right)\left(r^4 - \frac{4R^2r^2}{3} + \frac{R^4}{3}\right). \tag{22}$$

From the continuity equation

$$\frac{\partial}{\partial y}(\rho ru) + \frac{\partial}{\partial r}(\rho rv) = 0 \quad \text{and} \quad v(0, y) = 0, \tag{23}$$

the radial velocity distribution $v(r, y)$, which corresponds to the approximate axial velocity $u(r, y)$ may be found as:

$$\frac{v}{u_0} = \left(\frac{r^5}{R^4} - \frac{3r^3}{2R^2}\right)\frac{1}{\rho u_0}\frac{\partial(\rho\bar{u})}{\partial y}. \tag{24}$$

The density, ρ, in equations (22) and (24) may be found from equation (10) and the assumption that the gas mixture behaves as an ideal gas:

$$\rho = \frac{PM}{\bar{R}T} \text{ where } M = x_1M_1 + x_2M_2.$$

The radial velocity as determined by equation (24) should not be expected to satisfy all boundary conditions since the axial velocity is only an approximation and indeed $v(R, y)$ is not equal zero.

An example of the results of equation (22) appears in Fig. 8. Here it is seen that the predicted axial velocity may reach a minimum in the center of the cylinder. This is markedly different from the parabolic velocity profile ordinarily expected and suggests experimental verification.

EXPERIMENTAL STUDY

To conduct an experimental study a transparent diffusion chamber and channel are constructed of Plexiglas. The inside diameter of the diffusion chamber is 1 in. and the length 2 in. It is centered in the top of the channel which is 4 in. wide, 2 in. thick, and 30 in. long. Helium gas flows vertically into the top of the diffusion chamber through a thickness of filter paper while nitrogen flows in one end of the channel. The two gases are allowed to diffuse in the diffusion chamber and then exit through a $\frac{3}{8}$ in. hole at the opposite end of the channel into a 4 ft length of tubing to the atmosphere. The diffusion chamber has a flat machined into it, but this is not recommended because it reduces the apparent size of objects inside. The entire outside of the diffusion chamber is covered with black construction paper with the exception of a $\frac{1}{16}$ in. slit running axially and the flat machined on the diffusion chamber. This slit allows lighting of a plane passing through the centerline of the

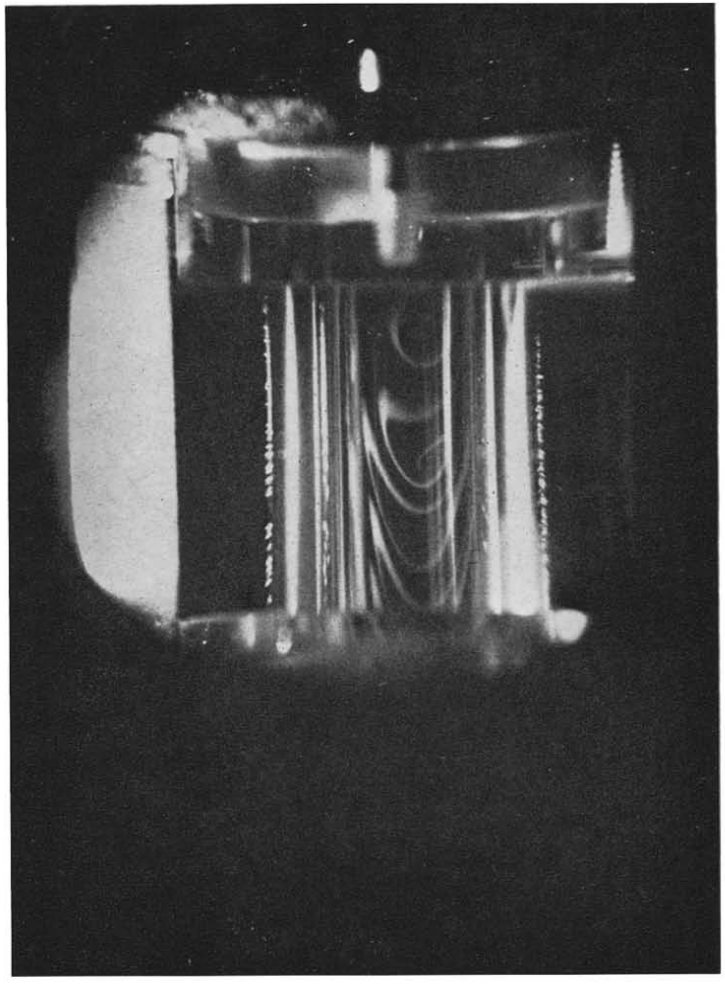

FIG. 2. Velocity profiles in cylindrical Diffusion Chamber (Smoke injection)—helium only.

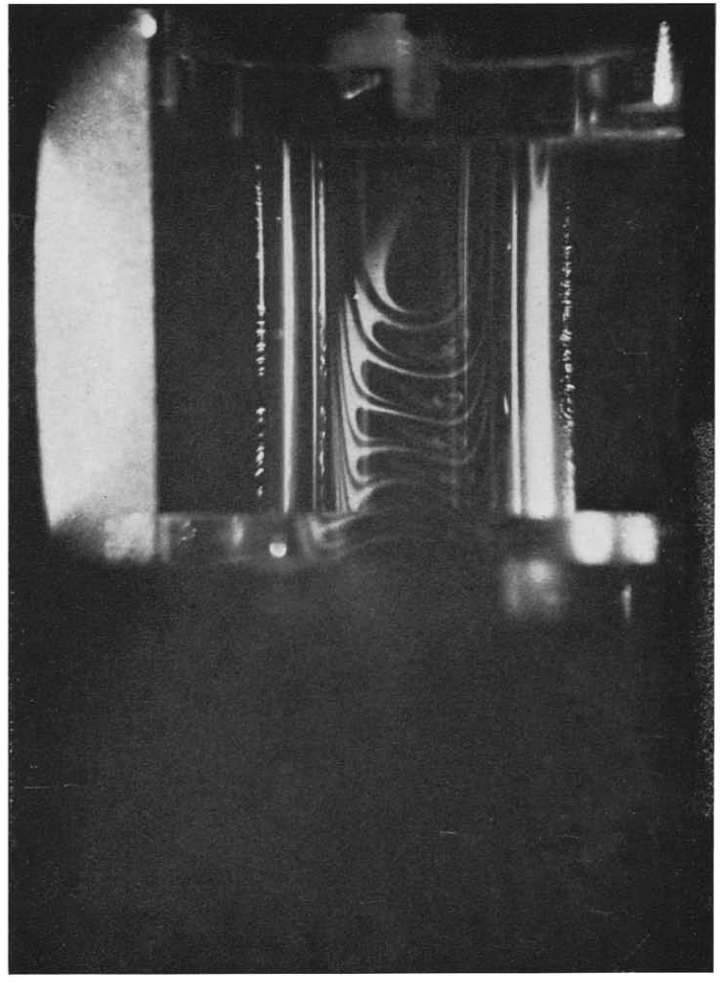

FIG. 3. Velocity profiles in cylindrical diffusion chamber (smoke injection)—helium in from top, nitrogen from right to left in channel.

[facing page 510]

chamber by a high intensity parallel beam light source.

This light source is necessary for illuminating pulses of smoke which are introduced by a probe through an opening in the diffusion chamber. This opening is located $\frac{1}{16}$ in. below the filter paper and lies in the incoming plane of light. The probe is made of 0·032 in. dia. stainless steel tubing and can be moved across the diameter of the diffusion chamber.

The smoke is obtained by burning oil saturated cigars with compressed air. The pulses are caused by allowing the smoke to flow through the probe for a few seconds, then stopping the flow, allowing the smoke in the diffusion chamber to exit and then squeezing the tubing leading to the probe to inject a small amount of smoke.

To verify the absence of flow disturbances or abnormalities a test is first run with helium admitted to the top of the diffusion chamber and no nitrogen flow. After this, a test with helium and nitrogen is observed. For the helium only test the gas is allowed to flow for approximately three hours before the test is begun to remove residual gases from the test section. The diffusion chamber is then illuminated for approximately 10 s while smoke is introduced, and a picture taken of the smoke pattern (Fig. 2). The expected parabolic velocity profile is produced.

For the second test the helium flow rate is adjusted as above ($F = 5$) and nitrogen is admitted to the channel. Again the diffusion chamber is illuminated for approximately 10 s and smoke introduced. The photograph (Fig. 3) shows that the axial velocity distribution is indeed not parabolic but rather reaches a minimum velocity in the center toward the bottom of the diffusion chamber.

To determine actual velocity profiles smoke injection is used in conjunction with an electrical timer. The timer is positioned adjacent to the diffusion chamber such that a picture may be taken of both simultaneously. The camera used is a Nikon-F 35 mm with a motor drive and appropriate extension tubes. There is distortion of the image of the illuminated plane on the actual film. This distortion is caused by the difference in index of refraction between air and the Plexiglas used for test section construction. The Plexiglas is cylindrical inside with a flat machined on the outside. To take this into consideration a picture is taken of a grid on a piece of cardboard which is placed inside the diffusion chamber. The grid is then removed and the tests begun without displacing the camera. This picture of the grid is then used

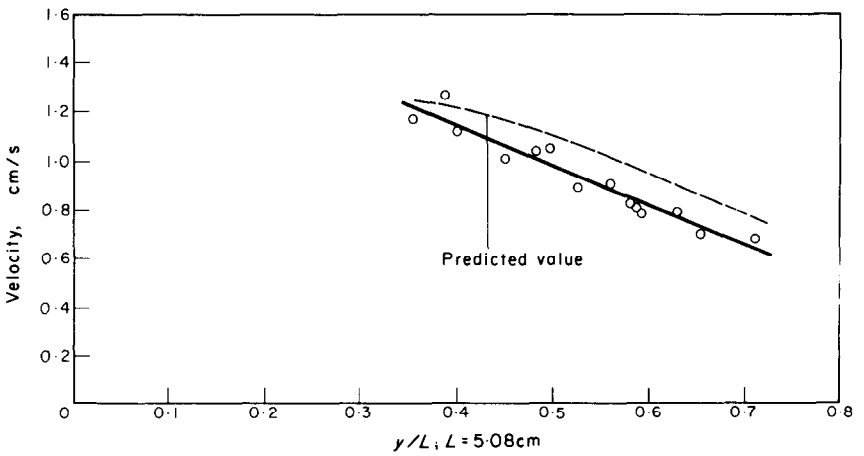

FIG. 4. Axial velocity as a function of axial distance at center line ($F = 5$).

later to obtain a scale factor between actual distances and distances on the film.

The actual velocities are determined by dividing the distance traveled by a smoke pulse by the elapsed time at various radial locations. The velocities determined by this method are then assigned to the midpoint of the distance traversed since the number obtained is an average over that distance.

The data taken as well as the predicted values are shown in Figs. 4–7. These figures show data at radial locations of centerline, $\pm 0{\cdot}2\ R$, $\pm 0{\cdot}4\ R$, and $+0{\cdot}6\ R$, respectively, with $R = 1{\cdot}27$ cm. Measurements are not presented closer to

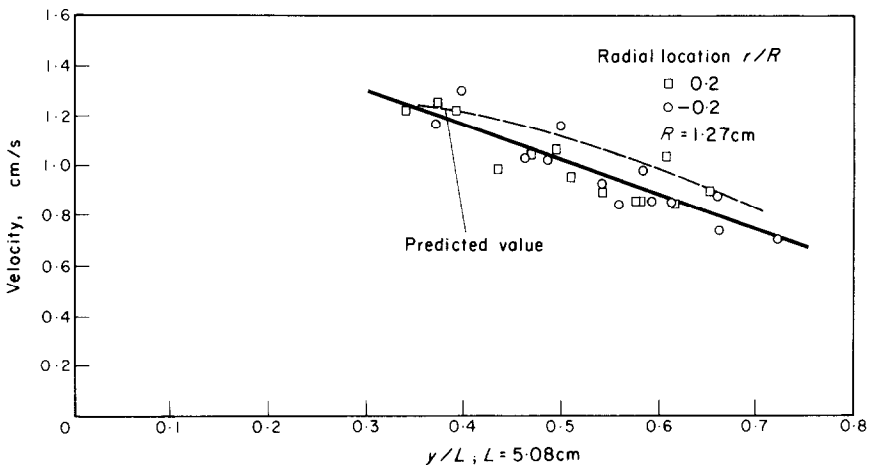

FIG. 5. Axial velocity as a function of axial distance $r/R = \pm 0{\cdot}2$, $(F = 5)$.

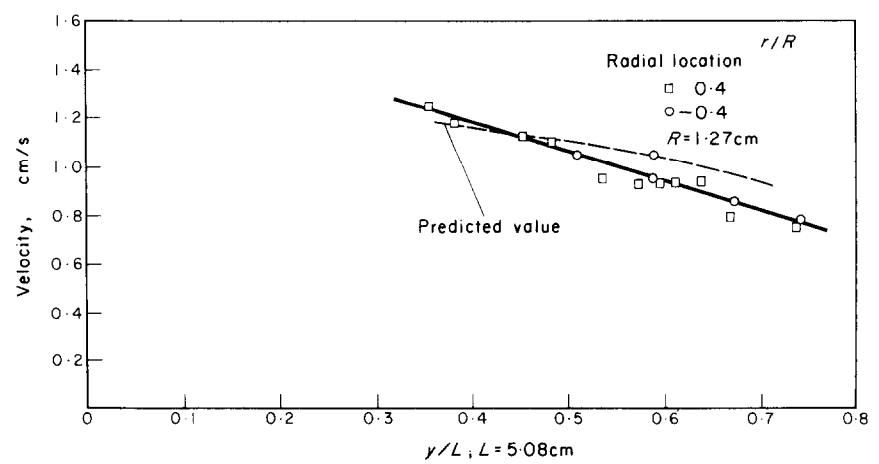

FIG. 6. Axial velocity as a function of axial distance, $r/R = \pm 0{\cdot}4$, $(F = 5)$.

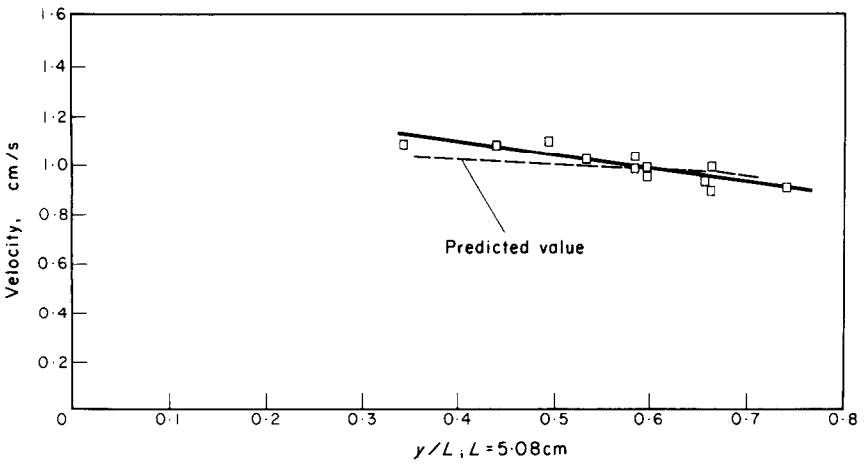

FIG. 7. Axial velocity as a function of axial distance, $r/R = +0{\cdot}6$, ($F = 5$).

the walls because the pulses of smoke tended to be smeared and distances could not be determined accurately. Radial velocities are not presented because they are smaller than the accuracy of the measurements in the regions in which they are measured.

ERROR ESTIMATE

The uncertainty in the experimental determination of the dimensionless parameter F is primarily due to the measurement of $\bar{m}_2$ and is estimated as ± 3 per cent. By calculation the uncertainty in the velocity should be less than 5 per cent but this number does not include the effects of free convection or the effects of gravity. In this case both the effects of gravity and free convection are important. Gravitational effects are important due to the difference in density of the pulses of smoke and the helium–nitrogen mixture in the diffusion chamber. This effect is minimized by using only small pulses of smoke. Free convection effects are important because of the intense light required in the diffusion chamber for photography. The light induced free convection effect causes velocities on the same order of magnitude as the diffusive velocity after only a few minutes. This effect is reduced greatly by using the light for only about 10 s at a time.

Even though these additional effects are reduced they are still present. Almost all of the data taken fall within ± 10 per cent of a straight line with the maximum deviation being 15 per cent.

It is suggested that for future experiments of this type that the accuracy of the experimental

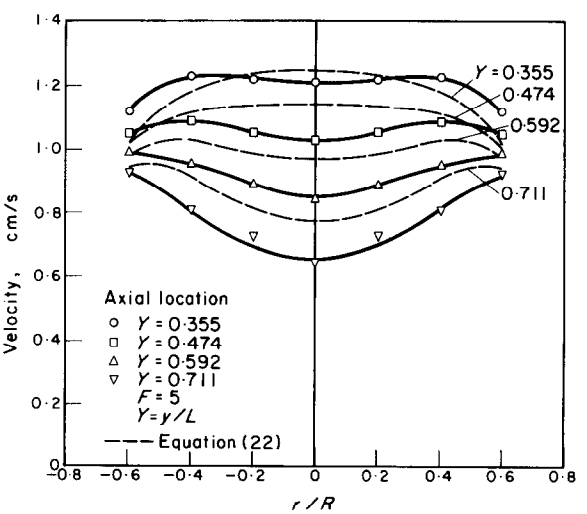

FIG. 8. Axial velocity for various axial locations (points from experimental graphs, $L = 5{\cdot}08$ cm, $R = 1{\cdot}27$ cm).

technique could be illuminated by comparing the experimentally determined velocity profile for the helium only test with a parabolic velocity profile. The theory should also be verified for other values of the parameter F.

CONCLUSION

The results of the axial measurements are summed in Fig. 8. It is seen that qualitatively the experimental measurements agree quite well with the predicted values. The velocities in Fig. 8 decrease in general with axial distance; the velocity profile is not parabolic, and toward the end of the diffusion chamber the velocity does reach a minimum along the center line. Quantitatively it should be noted that the experimental and predicted centerline velocities disagree by 20 per cent for $Y = 0{\cdot}711$. Also, there is no prediction of a dip at the 0·355 location, but one is found experimentally.

ACKNOWLEDGEMENT

Support for this research by the Office of Naval Research under Themis Contract N00014-68-A-0141-0001 is hereby gratefully acknowledged.

REFERENCE

1. E. N. SIEDER and C. E. TATE, Heat transfer and pressure drop of liquids in tubes, *Ind. Engng Chem.* **28**, 1429–1435 (1936).

PROFILS DE VITESSE DANS DEUX COURANTS GAZEUX INTERDIFFUSANTS

Résumé—On présente les profils expérimentaux de vitesse d'un écoulement dans un tube où apparaît un fort gradient de concentration pour un mélange de deux gaz. Pour des vitesses convective et diffusive ayant approximativement même grandeur, les profils de vitesse sont très nettement différents des profils paraboliques généralement supposés et ils peuvent présenter un minimum près de l'axe du tube. A partir de la théorie de diffusion de premier ordre, on utilise un profil de concentration avec des séries de puissance afin de réaliser une distribution approchée de vitesse axiale.

GESCHWINDIGKEITSPROFILE FÜR ZWEI INEINANDER DIFFUNDIERENDE GASSTRÖME

Zusammenfassung—Für eine Rohrströmung mit einem Zweistoff-Gasgemisch, in dem ein starker Konzentrationsgradient auftritt, werden experimentell ermittelte Geschwindigkeitsprofile dargestellt. Bei Konvektions- und Diffusionsgeschwindigkeiten von annähernd gleicher Grösse unterscheiden sich die Geschwindigkeitsprofile merklich von den gewöhnlich erwarteten parabolischen Profilen und können ein Minimum entlang der Rohrachse aufweisen. Um eine angenäherte axiale Geschwindigkeitsverteilung zu erhalten, wird ein Konzentrationsprofil aus der Reihenentwicklung einer Näherungstheorie erster Ordnung für die Diffusion benutzt.

ПРОФИЛИ СКОРОСТИ В ДВУХ ПОТОКАХ ГАЗА С ВЗАИМНОЙ ДИФФУЗИЕЙ

Аннотация—Представлены экспериментальные профили скоростей для потока в трубе с появляющимся градиентом сильной концентрации в бинарной газовой смеси. При конвективной и диффузионной скоростях приблизительно одной и той же величины профили скоростей значительно отличаются от обычно ожидаемых параболических профилей и могут достигать минимума в центре трубы. Используется профиль концентрации из теории диффузии первого порядка, представленный степенным рядом, для того чтобы получить приблизительное аксиальное распрделение скорости.